Sequence-Specific Knockdown of EWS-FLI1 by Targeted, Nonviral Delivery of Small Interfering RNA Inhibits Tumor Growth in a Murine Model of Metastatic Ewing's Sarcoma

Siwen Hu-Lieskovan, Jeremy D. Heidel, Derek W. Bartlett, et al.

Cancer Res 2005;65:8984-8992.

Sequence-Specific Knockdown of EWS-FLI1 by Targeted, Nonviral Delivery of Small Interfering RNA Inhibits Tumor Growth in a Murine Model of Metastatic Ewing's Sarcoma

Siwen Hu-Lieskovan,[1] Jeremy D. Heidel,[2] Derek W. Bartlett,[2] Mark E. Davis,[2] and Timothy J. Triche[1]

[1]Department of Pathology, Children's Hospital Los Angeles, Los Angeles, California and [2]Chemical Engineering, California Institute of Technology, Pasadena, California

Abstract

The development of effective, systemic therapies for metastatic cancer is highly desired. We show here that the systemic delivery of sequence-specific small interfering RNA (siRNA) against the *EWS-FLI1* gene product by a targeted, nonviral delivery system dramatically inhibits tumor growth in a murine model of metastatic Ewing's sarcoma. The nonviral delivery system uses a cyclodextrin-containing polycation to bind and protect siRNA and transferrin as a targeting ligand for delivery to transferrin receptor–expressing tumor cells. Removal of the targeting ligand or the use of a control siRNA sequence eliminates the antitumor effects. Additionally, no abnormalities in interleukin-12 and IFN-α, liver and kidney function tests, complete blood counts, or pathology of major organs are observed from long-term, low-pressure, low-volume tail-vein administrations. These data provide strong evidence for the safety and efficacy of this targeted, nonviral siRNA delivery system. (Cancer Res 2005; 65(19): 8984-92)

Introduction

Treatment-resistant metastases are the ultimate cause of death in most cancer patients. Ewing's family of tumors (EFT), a poorly differentiated mesenchymal malignancy that arises in bone or soft tissue, is a particularly cogent example. Historical data show that virtually all patients die from metastases (e.g., <5% survival after localized therapy; ref. 1). Systemic chemotherapy has markedly improved survival of patients with localized disease, but patients with metastatic disease rarely benefit (2). A major factor contributing to this outcome is the development of multidrug resistance by the time patients are treated for metastasis.

Specific chromosomal translocations are associated with numerous hematopoietic and solid tumors. The translocation t(11;22) is commonly detected in EFT and produces the chimeric *EWS-FLI1* fusion gene found in 85% of EFT patients (2). Functionally equivalent chimeric genes are found in virtually all EFTs (3). EWS-FLI1 is thought to be a transcriptional activator and plays a significant role in tumorigenesis of EFT (4, 5). Reduction of the EWS-FLI1 protein in EFT cells *in vitro* or in s.c. xenograft tumors by antisense oligonucleotides complementary to EWS-FLI1 mRNA results in decreased proliferation (6–8), suggesting a potential therapeutic intervention directed at this tumor-specific chimeric gene. Small interfering RNAs (siRNA) have recently been shown to silence the *EWS-FLI1* gene and suppress proliferation of an EFT cell line *in vitro* (9–11). We therefore hypothesized that systemically delivered siRNA against EWS-FLI1 would inhibit growth and dissemination of EFT cells *in vivo*.

Systemic applications of virally delivered siRNA and related RNA interference (RNAi) products are unlikely to be viable in the near future because of host immune responses on repeated delivery and ineffective tumor targeting. The systemic, nonviral delivery of RNAi molecules has been reported in mice and initially involved high-pressure, high-volume tail-vein injections of naked nucleic acid (12–14), a method untenable and unacceptable in humans in routine clinical settings. Subsequently, naked siRNA (15–17), lipid-formulated siRNA (18), plasmids expressing short hairpin RNA (19, 20), and polycation-formulated siRNA (21–23) have been given systemically in mice. Naked or formulated siRNAs have also been directly injected into xenograft tumors in mice (24–27). Naked siRNAs require chemical stabilization for *in vivo* use (17, 28), have nonspecific biodistributions that are the same as single-stranded antisense agents (29) and require large and repeated dosages for efficacy (17).

Some of us have been involved in the design and development of a nonviral delivery system specifically created for systemic use (30, 31). This multicomponent delivery system includes short polycations containing cyclodextrins that provide low toxicity and enable assembly with the other components of the delivery system that contain targeting ligands (Fig. 1). The cyclodextrin-containing polycations (CDP) self-assemble with siRNA to form colloidal particles ~50 nm in diameter, and their terminal imidazole groups assist in the intracellular trafficking and release of the nucleic acid (32). CDP protects the siRNA from degradation so that chemical modification of the nucleic acid is unnecessary. The colloidal particles are stabilized for use in biological fluids by surface decoration with polyethylene glycol (PEG) that occurs via inclusion complex formation between the terminal adamantane and the cyclodextrins; some of the PEG chains contain targeting ligands for specific interactions with cell-surface receptors (Fig. 1*A*). Here, we use transferrin as the targeting ligand (33) because tumor cells often overexpress the cell-surface transferrin receptor (34). The complete formulation of the siRNA-containing particles is done by mixing the components together and allowing for the self-assembly as schematically illustrated in Fig. 1*B*. A review of this delivery system is available (32). By using *in vivo*, whole-body fluorescence imaging, this system has been shown to deliver fluorescently labeled ssDNA to tumor cells in s.c., tumor-bearing nude mice from tail-vein injections (35). Absence of the transferrin ligand on the

Note: S. Hu-Lieskovan, J.D. Heidel, M.E. Davis, and T.J. Triche contributed equally to this work.

Supplementary data for this article are available at Cancer Research Online (http://cancerres.aacrjournals.org/).

Requests for reprints: Timothy J. Triche, Department of Pathology and Laboratory Medicine, Children's Hospital Los Angeles, Box 43, 4650 Sunset Boulevard, Los Angeles, CA 90027. Phone: 323-669-4516; Fax: 323-667-1123; E-mail: triche@usc.edu or Mark E. Davis, Chemical Engineering, California Institute of Technology, 1200 E. California Boulevard, Pasadena, CA 91125. E-mail: mdavis@cheme.caltech.edu.

doi:10.1158/0008-5472.CAN-05-0565

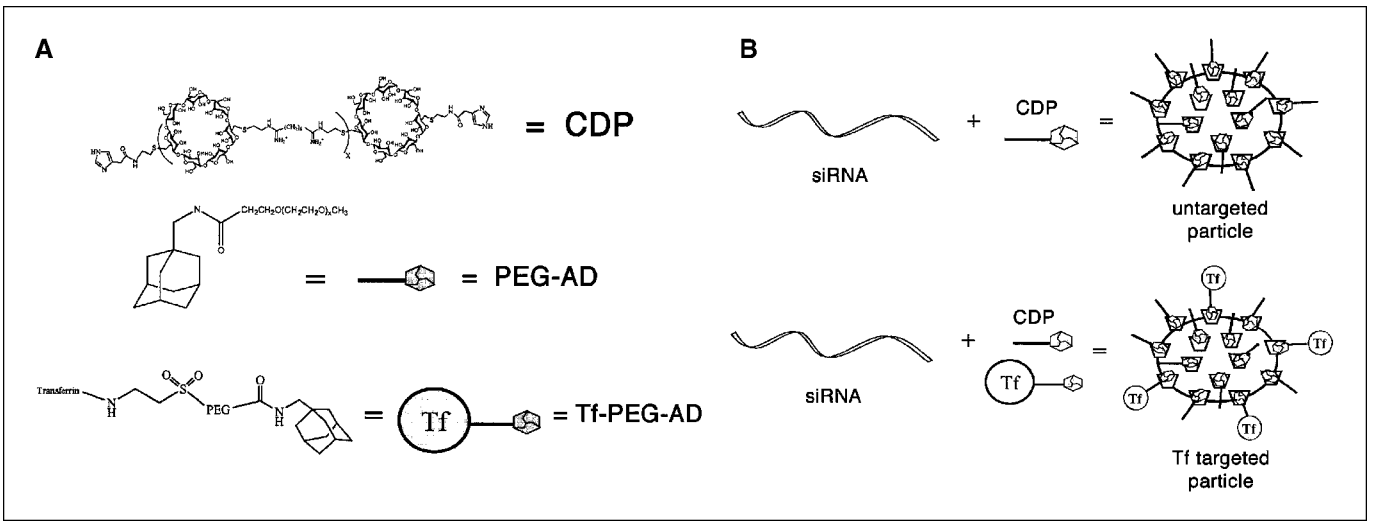

Figure 1. Schematic illustration of the delivery system. *A,* components of the delivery system. The CDP condenses siRNA and protects it from nuclease degradation. The AD-PEG conjugate stabilizes the particles in physiologic fluids via inclusion compound formation. The AD-PEG-transferrin (*Tf-PED-AD*) conjugate confers a targeting ligand to particles, promoting their uptake by cells overexpressing the cell-surface transferrin receptor. *B,* assembly of the nontargeted and targeted particles. For nontargeted particles, CDP and AD-PEG are combined and added to siRNA to generate stable but nontargeted polyplexes. For targeted particles, CDP, AD-PEG, and AD-PEG-transferrin are combined and added to siRNA to generate stable, targeted particles.

particles still provided tumor localization, but no uptake in tumor cells was observed (33, 35).

The safety of siRNA therapy in animals and ultimately humans has also been questioned, especially with regard to triggering IFN-mediated immune responses (36, 37). We recently showed that naked siRNA can be safely given to mice without eliciting an IFN response (38). Thus far, there are no studies of either the systemic, nonviral delivery of RNAi molecules in a metastatic tumor model or the investigation of the safety of nonviral, systemic administration of formulated siRNA. Here, we address both of these issues.

To show safe, systemic efficacy of nonvirally delivered siRNA, we first developed a mouse model of metastatic EFT in NOD/scid mice by tail-vein injections of EFT cells engineered to constitutively express luciferase. The fate of tumor cells was followed by *in vivo*, whole-body imaging. We tested the ability of targeted, nonviral delivery of siRNA against EWS-FLI1 to safely limit bulk metastatic tumor growth and prevent establishment of bulk metastatic disease from microscopic metastatic disease. We prove here the hypothesis that the targeted, nonviral delivery of siRNA can safely abrogate EWS-FLI1 expression and inhibit metastatic Ewing's tumor growth *in vivo*.

Materials and Methods

Small interfering RNA sequences. siRNA targeting luciferase (siGL3), the breakpoint of EWS-FLI1 (siEFBP2), a mutated negative control for siEFBP2 (siEFBP2mut), and a nontargeting control sequence (siCON1) were obtained from Dharmacon Research, Inc. (Lafayette, CO). All came purified and preannealed ("option C"). The sequences are siGL3: 5′-CUUACGCUGAGUACUUCGAdTdT and dTdTGAAUGCGACUCAUGAAGCU-5′, siEFBP2(9): 5′-GCAGAACCCUUCUUAUGACUU and UUCGUCUUGGGAAGAAUACUG-5′, siEFBP2mut(9): 5′-GCAGAACCAGUCUUAUGACUU and UUCGUCUUGGUCAGAAUACUG-5′, and siCON1: 5′-UAGCGACUAAACACAUCAAUU and UUAUCGCUGAUUUGUGUAGUU-5′.

***In vitro* down-regulation of EWS-FLI1 in an EFT cell line.** TC71 cells were grown on six-well plates in RPMI 1640 with 10% fetal bovine serum (FBS; no antibiotics) until they reached 30% confluency. siRNA was complexed with Oligofectamine (Invitrogen, San Diego, CA) according to the manufacturer's recommendations or with imidazole-terminated CDP at a 3:1 (+/−) charge ratio (32). The resulting formulations were applied to each well at a final concentration of 100 nmol/L. All transfected cells were harvested at 48 hours and gene expression was assessed by Western blot analysis. Primary monoclonal antibodies against the COOH-terminal region of FLI1 were obtained from BD Pharmingen, San Diego, CA. Polyclonal antibodies against β-actin were obtained from Santa Cruz Biotechnology (Santa Cruz, CA).

Determination of relative surface transferrin receptor level in TC71 cells. TC71, A2780, and HeLa (the latter two cell lines from American Type Culture Collection, Manassas, VA) cells were analyzed for relative levels of transferrin receptor expression. Cells were plated at 300,000 per well in six-well plates 24 hours before exposure to 1 mL antibiotic-free culture medium containing 1% bovine serum albumin and various concentrations of fluorescein-labeled transferrin as described previously (ref. 35; 50, 100, or 250 nmol/L) for 1 hour at 37°C. The cells were washed twice with PBS, collected by trypsin treatment, washed twice in fluorescence-activated cell sorting buffer (25 mL HBSS supplemented with 2 mmol/L $MgCl_2$ and containing 10 mL DNase), and resuspended in HBSS for analysis by flow cytometry using a FACSCalibur (Becton Dickinson, Franklin Lakes, NJ).

Transduction of TC71 cells with luciferase. SMPU-R-MNCU3-LUC is a lentiviral vector based on HIV-1 that transduces the firefly luciferase gene. The backbone vector SMPU-R has deletions of the enhancers and promoters of the HIV-1 long terminal repeat (SIN), has minimal HIV-1 *gag* sequences, contains the cPPT/CTS sequence from HIV-1, has three copies of the UES polyadenylation enhancement element from SV40, and has a minimal HIV-1 RRE [gift of Paula Cannon, Children's Hospital Los Angeles (CHLA), Los Angeles, CA; ref. 39]. The vector has the U3 region from the MND retroviral vector as an internal promoter driving expression of the firefly luciferase gene from SP-LUC+ (Promega, Madison, WI; ref. 40).

TC71 cells were transduced with viral supernatant containing SMPU-R-MNCU3-LUC vector (41). A second cycle of transduction was done 8 hours later by removing old medium and adding new virus supernatant and medium. Twenty-four hours after the initial transduction, cells were thoroughly washed thrice with PBS before *in vitro* analysis.

Injection of mice with luciferase-expressing TC71 cells. TC71-LUC cells were grown in RPMI 1640 with 10% FBS and antibiotics (penicillin/streptomycin). To prepare for injection, cells were trypsinized from the tissue culture flasks and washed twice with PBS. Cells were counted on a hemacytometer slide and resuspended in serum-free, antibiotic-free medium immediately before injection. The viability of the cells was tested by trypan blue exclusion. Only cells >90% viable were used.

Mice were treated according to the NIH Guidelines for Animal Care and as approved by the Caltech Institutional Animal Care and Use Committee. All mice were 6 to 8 weeks of age at the time of injection. Each mouse was injected with 5×10^6 TC71-LUC cells suspended in 0.2 mL RPMI (without FBS or antibiotics) through the tail vein using a 27-gauge needle. All experimental manipulations with the mice were done under sterile conditions in a laminar flow hood.

Bioluminescent imaging of the mice. After the injection of cells, the mice were imaged at different time points using an *in vivo* IVIS 100 bioluminescence/optical imaging system (Xenogen, Alameda, CA). D-Luciferin (Xenogen) dissolved in PBS was injected i.p. at a dose of 150 mg/kg 10 minutes before measuring the light emission. General anesthesia was induced with 5% isoflurane and continued during the procedure with 2.5% isoflurane introduced via a nose cone.

After acquiring photographic images of each mouse, luminescent images were acquired with various (1-60 seconds) exposure times. The resulting grayscale photographic and pseudocolor luminescent images were automatically superimposed by the IVIS Living Image (Xenogen) software to facilitate matching the observed luciferase signal with its location on the mouse. Regions of interest (ROI) were manually drawn around the bodies of the mice to assess signal intensity emitted. Luminescent signal was expressed as photons per second emitted within the given ROI. Tumor bioluminescence in mice is linearly correlated with the tumor volume (42, 43) and we have verified these findings (data not shown).

Formulation of nonviral, small interfering RNA–containing polyplexes for *in vivo* administration. All complexes were made with siRNA and an imidazole-modified CDP synthesized as described previously (31). Before addition to siRNA, CDP was mixed with an adamantane-PEG_{5000} (AD-PEG) conjugate at a 1:1 AD:β-CD (mol/mol) ratio. Targeted polyplexes also contained transferrin-modified AD-PEG (AD-PEG-transferrin) at a 1:1,000 AD-PEG-transferrin:AD-PEG (w/w) ratio. This mixture was then added to an equal volume of siRNA at a charge ratio (positive charges from CDP to negative charges from siRNA backbone) of 3:1 (+/−). An equal volume of 10% (w/v) glucose in water was added to the resulting polyplexes to give a final polyplex formulation in 5% (w/v) glucose (D5W) suitable for injection.

Consecutive-day delivery of small interfering RNA to tumors *in vivo*. Mice with successful tumor cell engraftment received injection of formulations containing siRNA against luciferase (siGL3), EWS-FLI1 (siEFBP2), or a control sequence (siCON1) on 2 or 3 consecutive days as indicated. Each mouse (~20 g) received 0.2 mL of the appropriate formulation, containing 50 μg siRNA corresponding to a 2.5 mg/kg dose, by low-pressure tail-vein injection using a 1 mL syringe and a 27-gauge needle.

Real-time quantitative reverse transcription-PCR. Total cellular RNA was isolated using RNA STAT-60 (Tel-Test, Friendswood, TX) from homogenized tumors. cDNA was synthesized from 2 μg DNase I (Invitrogen)–treated total RNA in a 42 μL reaction volume using oligo(dT) and SuperScript II (Invitrogen) for 60 minutes at 42°C following the supplier's instructions. PCR primers were designed with MacVector 7.0 (Accelrys, San Diego, CA). The sequences are EWS-FLI1: forward 5′-CGACTAGTTATGATCAGAGCAGT-3′ and reverse 5′-CCGTTGCTCTGTATTCTTACTGA-3′ and β-actin: forward 5′-GCACCCCGTGCTGCTGAC-3′ and reverse 5′-CAGTGGTACGGCCAGAGG-3′.

PCR was done as described before (44). PCR conditions were 95°C for 900 seconds; 40 cycles of 95°C for 15 seconds, 60°C for 30 seconds, and 72°C for 30 seconds; and a final denaturing stage from 60°C to 95°C. All PCR products were analyzed on 1% agarose gel and single band was observed, except negative controls. The reproducibility was evaluated by at least three PCR measurements. The expression level of target gene was normalized to internal β-actin and the mean and SD of the target/β-actin ratios were calculated for sample-to-sample comparison.

Long-term delivery of small interfering RNA to tumors *in vivo*. Fifty female NOD/scid mice were injected with 5×10^6 TC71-LUC cells as described above. Immediately after cell injection, each mouse received an additional injection of 0.2 mL of one of the following formulations (concentrations indicated above, 10 mice per group): D5W only (group A); naked siEFBP2 only (group B); targeted, formulated siCON1 (group C); targeted, formulated siEFBP2 (group D); or nontargeted, formulated siEFBP2 (group E). Formulations were given twice weekly for 4 weeks. Images were taken immediately after the first injections for quality control of the injections and twice weekly immediately before the injection of the formulations. We continued to monitor the tumor signal in the mice receiving targeted (group D) and nontargeted (group E) siEFBP2 formulations for an additional 3 weeks or until the tumor burden was too great for the mice.

Magnetic resonance imaging. Before imaging, each mouse received 100 μL paramagnetic contrast agent Magnevist (1 mL Magnevist contains 469.01 mg gadopentate dimeglumine, 0.99 mg meglumine, and 0.4 mg diethylenetriamine pentaacetic acid) i.p. to enhance delineation. Mice were sedated with 5% isoflurane and wrapped in cellophane to prevent hypothermia and minimize contamination of the magnetic resonance imaging (MRI) system. Isoflurane gas (0.8% in air) was used for supplementary sedation as needed. All images were obtained using a Bruker BioSpin MRI with a horizontal magnet of 7.0 Tesla (Bruker Instruments, Inc., Billerica, MA).

Toxicity, immune response, and pathology studies. Female C57BL/6 mice (The Jackson Laboratory, Bar Harbor, ME) were 6 to 8 weeks of age at the time of injection. To measure plasma cytokine levels, blood was harvested from mice 2 and 24 hours after injection by cardiac puncture and plasma was isolated using Microtainer tubes (Becton Dickinson). Whole blood was used for complete blood count (CBC) analyses, and plasma was used for all liver enzyme and cytokine analyses. Interleukin (IL)-12 (p40; BD Biosciences) and IFN-α levels (PBL Biomedical Laboratories, Piscataway, NJ) were measured by ELISA according to the manufacturer's instructions.

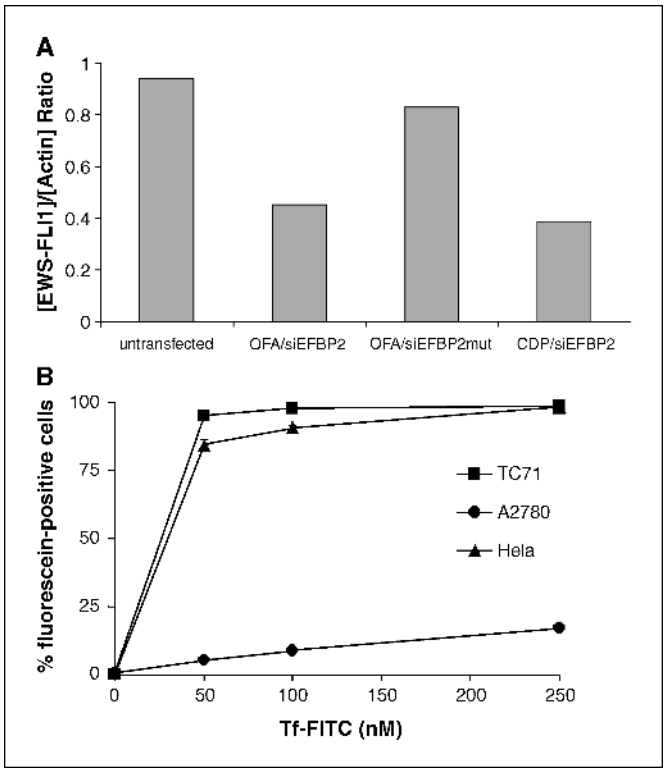

Figure 2. *In vitro* down-regulation of EWS-FLI1 in cultured TC71 EFT cells. *A,* quantification of Western blot analysis. Cultured TC71 cells were exposed to siEFBP2-containing formulations made with Oligofectamine (*OFA*) or CDP for 4 hours. At 48 hours after transfection, cells were lysed and total cell protein was denatured, electrophoresed, and transferred to a polyvinylidene difluoride membrane that was probed with antibodies to EWS-FLI1 or actin (siEFBP2mut: mutant negative control). Average band intensities were determined by densitometry and the ratio of EWS-FLI1 to actin intensities was calculated. *B,* determination of the relative surface transferrin receptor level in TC71 cells. Cultured TC71 cells were incubated in medium containing fluorescein-labeled transferrin; uptake was assessed by flow cytometry. This experiment was also done on cell lines known to express high and low levels of transferrin receptor (HeLa and A2780, respectively) for comparison.

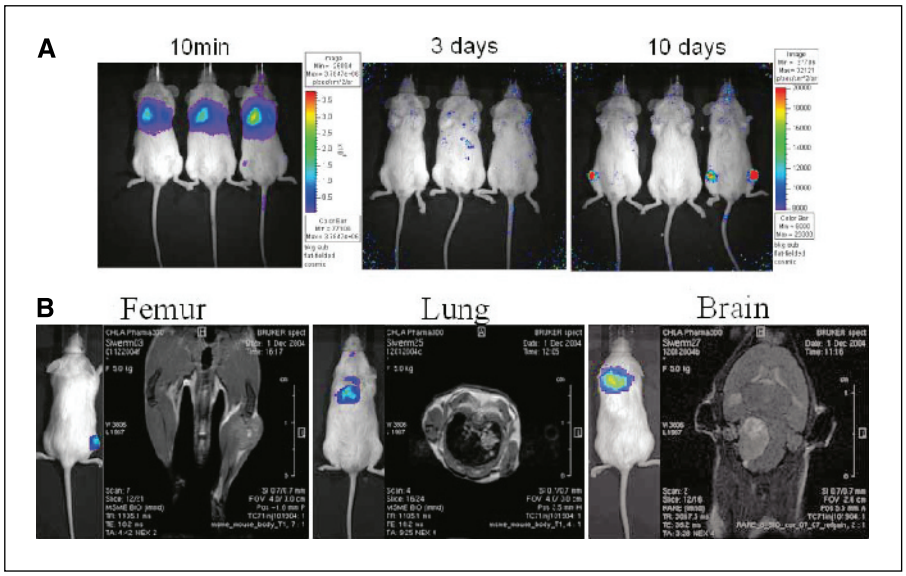

Figure 3. Establishment of a metastatic EFT model in mice. *A,* NOD/scid mice injected with TC71-LUC cells developed metastatic tumors. Mice were injected with TC71-LUC cells via the tail vein. At various time points after injection, mice were anesthetized, injected with D-Luciferin, and imaged using a Xenogen IVIS 100 bioluminescence imaging system. *B,* MRI confirmation of EFT engraftments. Tumor-bearing mice were anesthetized, injected with contrast agent, and imaged. Tumor locations observed by MRI corresponded to bioluminescent signal.

Major organs of the NOD/scid mice after long-term treatment studies were collected, formalin fixed, and processed for routine H&E staining using standard methods. Images were collected using a Nikon (Japan) epifluorescent microscope with a DP11 digital camera.

Results

Small interfering RNA mediates down-regulation of EWS-FLI1 in cultured TC71 EFT cells. RNAi-mediated gene silencing in TC71, an EFT cell line that expresses the *EWS-FLI1* fusion gene, was assessed using a commercial lipid reagent (Oligofectamine) and our imidazole-terminated CDP. Using a previously reported siRNA sequence targeting the EWS-FLI1 breakpoint (siEFBP2; ref. 9), we observed comparable and significant (>50%) reduction in EWS-FLI1 protein levels with both delivery methods (Fig. 2*A*). Delivery of a mutant siRNA sequence (siEFBP2mut) failed to elicit such down-regulation.

TC71 cells display a high relative surface transferrin receptor level. The level of the cell-surface transferrin receptor in TC71 cells was determined relative to cell lines shown previously to have high (HeLa) and low (A2780) transferrin receptor levels (ref. 35; Fig. 2*B*). By 50 nmol/L concentration, we observed 100% uptake of a FITC-transferrin conjugate by TC71 cells, even higher than that by HeLa cells at all FITC-transferrin concentrations examined. These results suggest that modification of siRNA formulations to contain a ligand for transferrin receptor could lead to successful targeting to TC71 cells *in vivo*.

Establishment of a murine model of metastatic Ewing's sarcoma. Luciferase-expressing TC71 cells (TC71-LUC) were generated by viral transduction and given to female NOD/scid mice by tail-vein injection. The pattern of TC71-LUC cell engraftment was assessed by acquiring serial images of *in vivo* bioluminescence for 5 to 8 weeks after transplantation. Signals could be detected immediately after the transplantation. Ten minutes after cell injection, the luminescence signals accumulated in the lung area, indicative of entrapment of TC71-LUC cells within the capillary bed of the lung (Fig. 3*A*). Over the next few hours, the bioluminescent signal gradually disappeared as the cells dispersed and reemerged 1 to 2 weeks later at various locations where tumors developed. The most common engraftment sites were lung, vertebral column, pelvis, femur, and soft tissue, similar to the most frequently observed sites for metastases in EFT patients (45). The locations of the engraftments were confirmed by MRI (Fig. 3*B*), computed tomography, X-ray scans, and necropsy with histopathologic confirmation (data not shown).

Formulated small interfering RNA against luciferase transiently reduces the bioluminescent signal of engrafted tumors *in vivo*. To test whether targeted, systemic CDP-mediated delivery of siRNA could provide gene silencing *in vivo*, two consecutive daily treatments (days 40 and 41 after cell injection) were done on mice bearing luciferase-producing metastasized EFT. The tumors of mice treated with the targeted, formulated siGL3-containing polyplexes showed a strong decrease (>90%) in luciferase signal 2 to 3 days after injection (Fig. S2). The luciferase down-regulation was transient. The luminescent signal increased daily thereafter. Heidel et al. have shown that low-volume tail-vein injections of naked siRNA at 2.5 mg/kg do not give luciferase down-regulation in mice most likely due to the lack of cellular uptake of naked siRNAs given at that dose (32). Taken together, these studies show that the transferrin-targeted, CDP-containing particles can deliver functional siRNA to TC71-LUC tumors when given via standard low-pressure tail-vein injection.

Formulated small interfering RNA against EWS-FLI1 inhibits tumor growth *in vivo*. Mice with successful engraftment of TC71-LUC cells were randomly selected for treatment with targeted, formulated siEFBP2 on days 35 to 37 after cell injection. Increases in bioluminescent signal from metastasized tumor growth were inhibited by systemic administration of targeted formulations containing siRNA against EWS-FLI1 (siEFBP2; Fig. 4*A*). Three consecutive daily injections of the targeted, formulated siEFBP2 resulted in a decreased tumor signal, and this effect lasted 2 to 3 days. Further assessment of the EWS-FLI1 expression in the tumors treated with two consecutive siEFBP2 formulations showed a 60% down-regulation of EWS-FLI1 RNA level compared with siCON1-treated tumors ($P = 0.046$; Fig. 4*B*). Therefore, the delivery of fully formulated siEFBP2 is able to reduce EWS-FLI1 expression in the established tumors and provide transient inhibition of EFT tumor growth.

Long-term, twice-weekly administration of targeted, formulated siEFBP2 inhibits tumor cell engraftment. After observing

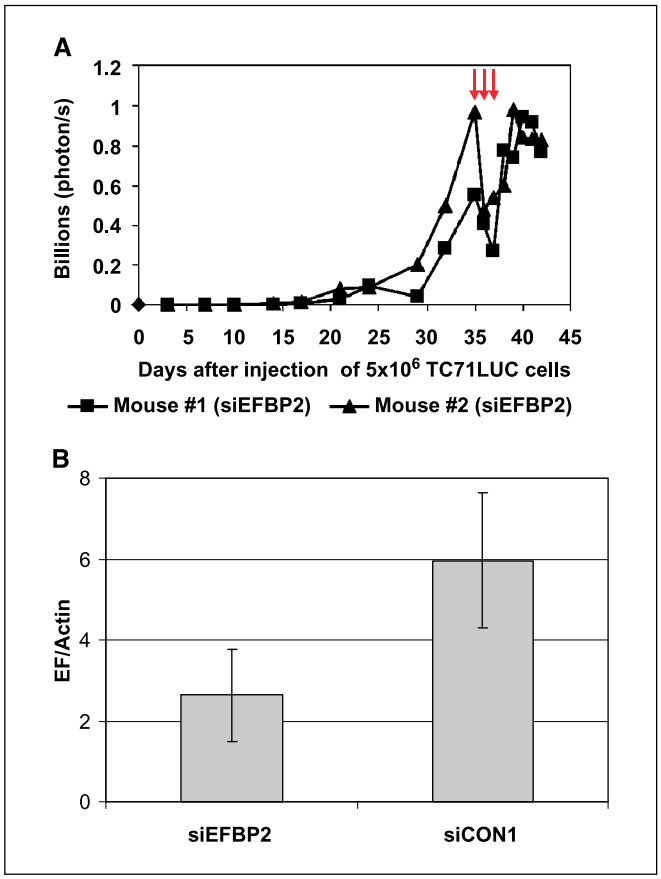

Figure 4. Effect of siEFBP2 formulations on growth of metastasized EFT in mice. *A,* reduced bioluminescence in mice receiving formulated siRNA targeting EWS-FLI1 (siEFBP2). siEFBP2 was formulated and targeted as described in Fig. 1 and given by low-pressure tail-vein injection on 3 consecutive days (days 35-37; *red arrows*) after injection of TC71-LUC cells. Transient reduction in bioluminescence was observed on days 36 and 37. *B,* EWS-FLI1 RNA level in tumors after two consecutive injections of fully formulated siRNA. Formulated siEFBP2 or siCON1 were given by low-pressure tail-vein injection on 2 consecutive days (days 19 and 20) after injection of TC71-LUC cells. Tumors were harvested on the third day. RNA were extracted and EWS-FLI1 level was determined by real-time quantitative reverse transcription-PCR.

transient effects *in vivo* after short-term (one to three daily treatments) administration of targeted siRNA formulations, we employed a long-term treatment regimen in which formulations were given twice weekly beginning the same day as injection of TC71-LUC cells. These studies allowed for the more careful investigation of the effects of the formulations that included all of the proper controls. The success of tumor cell injection was confirmed by imaging mice immediately after the injection (Fig. S1). Targeted, formulated siEFBP2 treatments (group D) dramatically inhibited the engraftment of TC71-LUC cells (Fig. 5*A* and *B*), with only 20% of the mice showing any tumor growth compared with 90% to 100% in other treatment groups (Fig. 5*A*). Neither the mice receiving naked siEFBP2 (group B) nor those receiving targeted delivery of siCON1 (group C) showed any difference in tumor engraftment compared with the control group that received only the 5% glucose carrier solution (D5W, group A). Interestingly, tumors in mice treated with formulated but nontargeted (lacking transferrin) siEFBP2 showed a delayed progression of tumor engraftment compared with the control groups (Fig. S1). Once significant tumors were established, however, the tumors seemed to grow at a rate unaffected by continued treatment with the nontargeted siEFBP2 (Fig. 5*B*). The tumor signal was monitored in the mice receiving targeted (group D) and nontargeted (group E) siEFBP2 formulations for an additional 3 weeks or until the tumor burden was too great for the mice. Whereas most of the mice receiving nontargeted formulations developed very large tumors, the majority of the mice receiving targeted formulations showed little or no tumor signal (Fig. 5*B*). We conclude that treatment with the targeted formulation of siEFBP2 prevented the tumor cell engraftment in these mice and slowed the growth of any tumors that did develop. In addition, targeted, formulated siEFBP2 complexes do not seem to cross the blood-brain barrier because the tumor growth of a brain metastasis treated by this complex was unaffected (Fig. S3). This result is consistent with previously reported biodistribution studies (35).

No immune response or major organ damage was observed after targeted, formulated siEFBP2 treatment in mice. Because the ability of the NOD/scid mice to mount a possible immune response to these formulations is severely compromised, single tail-vein injections of formulations were repeated in immunocompetent mice (C57BL/6) and blood was collected at 2 or 24 hours after the injections. CBCs of whole blood showed insignificant changes in WBC or platelet counts (Fig. 6*A*). Levels of secreted liver enzymes [aspartate aminotransferase (AST) and alanine aminotransferase (ALT)], blood urea nitrogen (BUN), and creatinine were all unchanged, indicating a lack of damage to the liver or kidneys. No increases, resulting from formulations, in plasma IL-12 or IFN-α at either 2 or 24 hours after injection were observed (Fig. 6*B*). We also did pathologic examination of the major organs (liver, kidney, brain, heart, lung, and pancreas) from the NOD/scid mice that received long-term treatments by H&E staining (Fig. 6*C*). No organ damage was observed with any of the formulated groups when compared with the D5W and naked siEFBP2 treatment groups. Taken together, these results show the safety and low immunogenicity of these CDP-containing formulations.

Discussion

The silencing of gene expression by siRNA is a powerful tool for the genetic analysis of mammalian cells and has the potential for development into specific, potent, and safe treatments for human disease. However, delivery of siRNA into specific organs *in vivo* is a major obstacle for RNAi-based therapy. To overcome this problem, a hydrodynamic method (high-pressure, high-volume tail-vein injection) has been used in mice to deliver siRNA (and other types of nucleotides) to the liver. This method is ineffective for other organs and is not feasible for routine clinical application (14, 46). Naked siRNA has been employed in mice but requires costly chemical stabilization and large, frequent dosing for efficacy (17). Although researchers have also shown successful viral delivery of plasmids to achieve prolonged and stable expression of siRNA (47–51), the immunogenicity of viral vectors provide significant barriers to their clinical use. In addition, it is difficult to influence the biodistribution of viral vectors and preferentially target tumor when given systemically. Therefore, the development of a targeted, nonimmunogenic siRNA delivery system for systemic administration is highly desired and will likely be required for effective use of siRNA as a human therapy. Here, we show that a cyclodextrin-based polycation delivery system (Fig. 1*A*) can be formulated (Fig. 1*B*) to target metastatic cancer in a murine model of the EFT.

We established a highly reproducible and clinically relevant metastatic murine model for the EFT in NOD/scid mice (Fig. 3).

EFT cells were transduced with the firefly luciferase gene before administration in mice, thus allowing for noninvasive, *in vivo*, whole-body imaging of bioluminescence to monitor the fate of tumor cells. The tumor engraftment sites observed (lung, vertebral column, pelvis, femur, and soft tissue) were comparable with the most common locations of metastases in EFT patients.

siRNA duplexes targeting the *EWS-FLI1* fusion gene (siEFBP2) or the firefly luciferase gene (siGL3) were formulated with the synthetic delivery system as schematically illustrated in Fig. 1. Because the TC71 cells used here were shown to express high levels of cell-surface transferrin receptors (Fig. 2*B*), targeted formulations contained transferrin as the targeting ligand. This delivery system self-assembles with siRNA to give ~50 nm particles that are stable

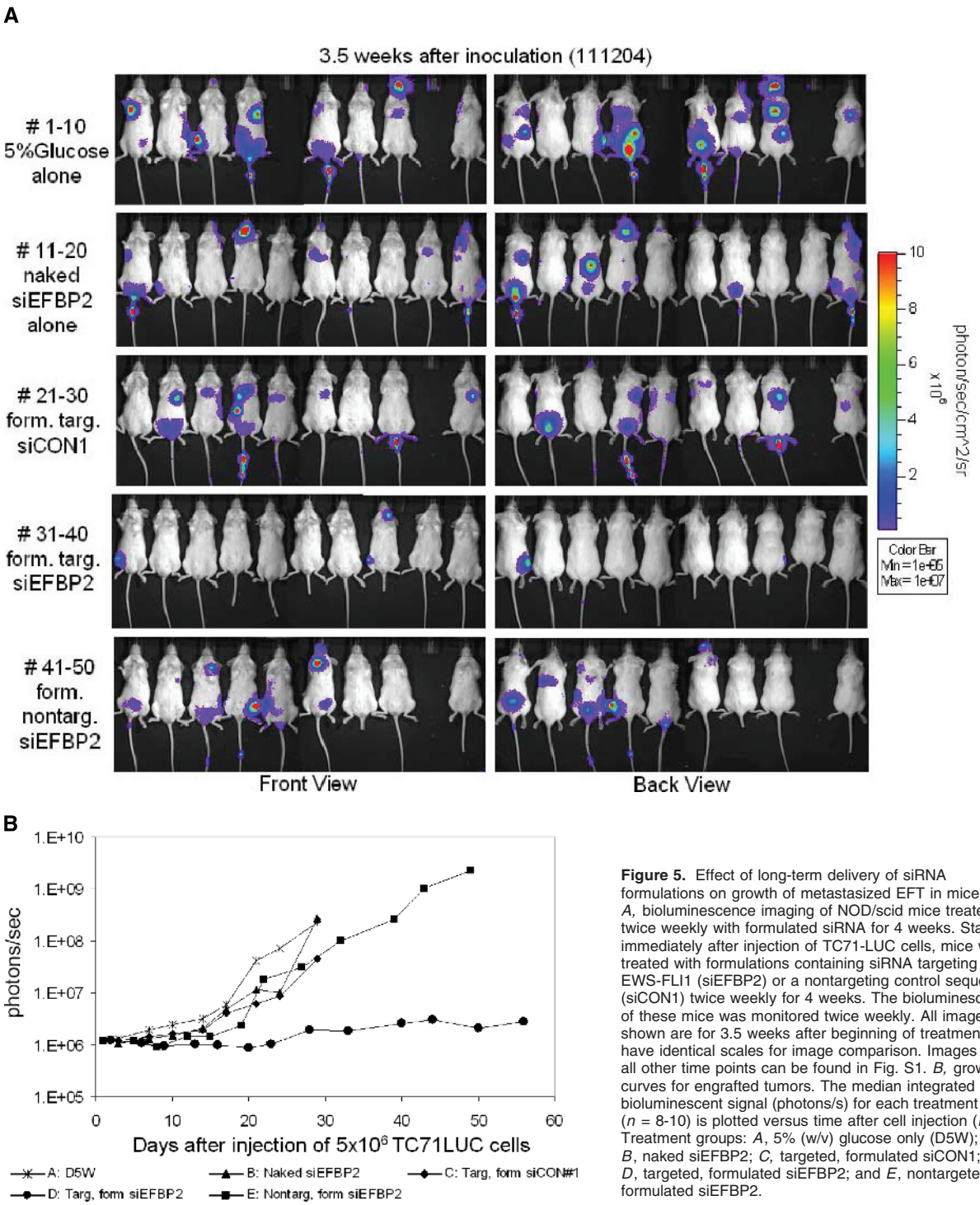

Figure 5. Effect of long-term delivery of siRNA formulations on growth of metastasized EFT in mice. *A,* bioluminescence imaging of NOD/scid mice treated twice weekly with formulated siRNA for 4 weeks. Starting immediately after injection of TC71-LUC cells, mice were treated with formulations containing siRNA targeting EWS-FLI1 (siEFBP2) or a nontargeting control sequence (siCON1) twice weekly for 4 weeks. The bioluminescence of these mice was monitored twice weekly. All images shown are for 3.5 weeks after beginning of treatment and have identical scales for image comparison. Images for all other time points can be found in Fig. S1. *B,* growth curves for engrafted tumors. The median integrated tumor bioluminescent signal (photons/s) for each treatment group (n = 8-10) is plotted versus time after cell injection (*D*). Treatment groups: *A*, 5% (w/v) glucose only (D5W); *B*, naked siEFBP2; *C,* targeted, formulated siCON1; *D*, targeted, formulated siEFBP2; and *E*, nontargeted, formulated siEFBP2.

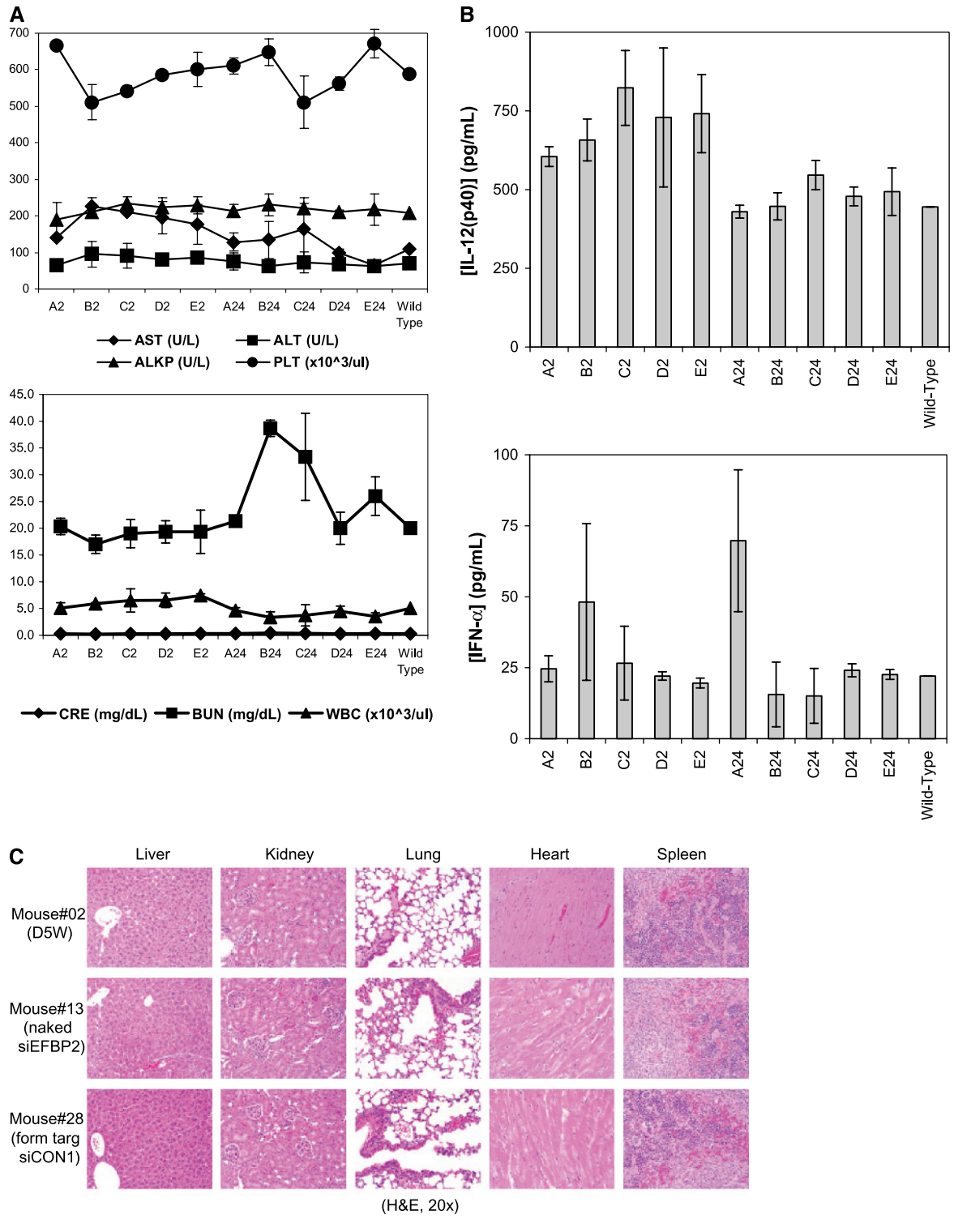

Figure 6. Formulated siRNA failed to exhibit toxicity or elicit an immune response in mice. *A,* CBC and liver panel results for C57BL/6 mice receiving formulations showed no toxicity or immune response. Female C57BL/6 mice received a single administration of formulated siRNA. At 2 or 24 hours after treatment, blood was drawn by cardiac puncture and plasma was isolated. Whole blood was used for determination of platelet and WBC counts. Plasma was used for measurement of AST, ALT, alkaline phosphatase (*ALKP*), creatinine, and BUN. *Points,* averages of triplicate mice for each time point; *bars,* SDs. *B,* cytokine ELISA results for C57BL/6 mice receiving formulations showed no up-regulation of IL-12 or IFN-α. The plasma levels of IL-12 (p40) and IFN-α in mice described above were measured by ELISA. Treatment groups: A, 5% (w/v) glucose only (D5W); B, naked siEFBP2; C, targeted, formulated siCON1; D, targeted, formulated siEFBP2; E, nontargeted, formulated siEFBP2; Wild Type, uninjected; 2, blood drawn 2 hours after injection; 24, blood drawn 24 hours after injection. *C,* H&E staining of major organs of the NOD/scid mice after long-term treatment. Major organs were collected, formalin fixed, and processed for routine H&E staining using standard methods. Images were collected using a Nikon epifluorescent microscope with a DP11 digital camera.

in physiologic fluid, can protect the nucleic acid from nuclease degradation (protection for at least 72 hours; data not shown), are capable of providing for cellular uptake and delivery of functional siRNA (Fig. 2*A*), and can target transferrin receptor–expressing tumor cells from tail-vein administration in mice (32–36). When introduced systemically into tumor-bearing mice by tail-vein injection, these formulations containing either siEFBP2 or siGL3 are able to achieve transient reduction in tumor growth or luciferase expression, respectively (Fig. 4; Fig. S2). The tumor growth inhibition was correlated with a sequence-specific down-regulation of EWS-FLI1 expression in the tumors.

Clinically, many tumors relapse after intensive treatment because of systemic dissemination of micrometastases. Nearly all EFT patients already have micrometastases at diagnosis, resulting in a >95% relapse rate when treated locally (1) and a 40% relapse rate after systemic chemotherapy (2). Therefore, effective treatment for elimination of circulating or dormant metastasized tumor cells after traditional therapy is needed. We explored the possibility of using targeted, formulated siRNA for this purpose by administration of formulations twice weekly beginning the same day as injection of TC71-LUC cells. These injections of the different formulations in tumor-bearing NOD/scid mice reveal that only the targeted, formulated siEFBP2 achieves long-term tumor growth inhibition (Fig. 5). Neither naked siEFBP2 nor a formulated control siRNA sequence shows any effect on tumor signal compared with the control group receiving only the carrier fluid. These results show the necessity of the delivery vehicle for systemic application and the sequence specificity of the observed inhibition.

Notably, mice treated with formulated but nontargeted siEFBP2 show an initial delay in tumor growth. However, the growth rate of tumors that eventually developed are unaffected by continuation of this treatment. The enhanced permeability and retention effect (EPR) leads to the accumulation of macromolecules in solid tumors (52). The leaky vasculature associated with the nascent tumors allows circulating targeted and nontargeted particles to accumulate in tumors. However, only the transferrin-containing, targeted particles were detected within tumor cells by fluorescence (35). Some small fraction of the nontargeted particles may have entered tumor cells. If so, their amount was below the detection limit. Mice receiving nontargeted formulations in the present study eventually develop very large tumors, whereas little or no tumor signal is observed by imaging or at autopsy in most mice receiving the targeted formulations. These results support the notion that transferrin targeting increases overall uptake of the nanoparticles through receptor-specific endocytosis by tumor cells after accumulation in the tumor mass via the EPR effect has occurred.

We hypothesize that treatment with the targeted formulation of siEFBP2 assists in the prevention of the initial establishment of tumors in these mice from the injected cells and slows the growth of any tumors that develop by down-regulating the expression of the oncogenic fusion protein EWS-FLI1. Because the siGL3-containing formulations show potent, sequence-specific down-regulation of *in vivo* bioluminescence, it is clear that the delivered siRNA is functional. Although the luciferase down-regulation is a direct observation of *in vivo* RNAi, the reduced tumor engraftments from siEFBP2-containing formulations require a more extended cascade of down-regulation and intracellular signal transduction events and are therefore indirect, but biologically significant, measures of sequence-specific RNAi.

Most of the tumor engraftment sites in the mouse model match those commonly seen in EFT-bearing patients. We also observed brain metastases, analogous to that rare event in human EFT patients (Figs. 3*B* and 5*A*). As expected, previous work with this delivery system showed that these formulations are unable to cross the blood-brain barrier (35), and as such, we would not expect them to reduce growth of brain metastases. Indeed, the targeted, formulated siEFBP2 complexes did not seem to affect the tumor growth of the illustrated brain metastasis (Fig. S3).

Recent *in vitro* reports have shown that siRNA sequences and their method of delivery may trigger an IFN response (36, 37). Additionally, *in vivo* delivery of siRNA by lipids have resulted in potent IFN responses (53–55). Here, single tail-vein injections of all of the formulations were done in immunocompetent (C57BL/6) mice to enable measurement of numerous blood markers that are indicative of an immune response. In contrast to results obtained from the injection of polyriboinosinic-polyribocytidylic acid, a known immunostimulator through interactions with Toll-like receptor 3 (38), none of the formulations show any significant effects on the levels of IL-12, IFN-α, WBC, platelets, secreted liver enzymes (ALT and AST), BUN, or creatinine (Fig. 6). All of these observations with formulated siRNA are consistent with our previous work showing a lack of immune response to naked siRNA (38). The cyclodextrin-based delivery system does not produce an IFN response even when siRNA is used that contains a motif known to be immunostimulatory when delivered *in vivo* with lipids (ref. 54; published sequence is within siCON1). These results show the safety and low immunogenicity of CDP-containing formulations and show the attractiveness of this methodology for systemic, targeted delivery of nucleic acids. The *in vivo* gene silencing effect of siRNA by our delivery system is transient, permitting fine-tuning of the intensity and interval of the treatment. For example, the frequency of administration can be tuned for use in combination with other agents, and the treatment can be terminated within a few days if necessary.

To our knowledge, this is the first study to show that systemic administration of siRNA can provide safe, sequence-specific inhibition of tumor growth in a disseminated tumor model. In contrast to naked siRNA delivery, the targeted siRNA formulations used here are efficacious at low siRNA doses and do not require chemical modification of the siRNA for stabilization. Further, this delivery system can be easily tuned to target different cell-surface receptors in tumors and other tissue (32), can be used to deliver different and/or multiple siRNA sequences, and does not elicit a detectable immune response or any changes in mouse physiology. We believe that this treatment has the potential to be developed into a useful method for inhibition of metastatic EFT growth and may also have broad applicability in cancer therapy. Future experiments using an EFT-specific targeting ligand and employing formulation combinations with small-molecule drugs will likely further enhance the antitumoral potency of this system.

Acknowledgments

Received 2/17/2005; revised 6/9/2005; accepted 7/6/2005.

Grant support: Molecular Genetics and Molecular Pathology from Las Madrinas at CHLA (S. Hu-Lieskovan), Whitaker Foundation doctoral fellowship (J.D. Heidel), and National Science Foundation graduate research fellowship (D.W. Bartlett).

The costs of publication of this article were defrayed in part by the payment of page charges. This article must therefore be hereby marked *advertisement* in accordance with 18 U.S.C. Section 1734 solely to indicate this fact.

We thank Greg Jensen (Insert Therapeutics, Inc., Pasadena, CA) for measurement of cellular transferrin receptor levels, Hu Wong (CHLA Clinical Laboratory) for CBC and liver panel analyses, Dr. Donald B. Kohn and Denise Petersen (CHLA Vector Core) for transduction of the TC71 cells, Dr. Hiroyuki Shimada and Minerva Mongeotti (CHLA Experimental Pathology Core) for processing of mouse autopsy tissues, and Dr. Rex Moats, Gevorg Karapetyan, and Ira Harutyunyan (CHLA Imaging Core) for the MRI studies.

References

1. Dahlin DC, Coventry MB, Scanlon PW. Ewing's sarcoma. A critical analysis of 165 cases. Am J Orthop 1961;43-A:185–92.
2. Rodriguez-Galindo C, Spunt SL, Pappo AS. Treatment of Ewing sarcoma family of tumors: current status and outlook for the future. Med Pediatr Oncol 2003;40:276–87.
3. Delattre O, Zucman J, Melot T, et al. The Ewing family of tumors—a subgroup of small-round-cell tumors defined by specific chimeric transcripts. N Engl J Med 1994;331:294–9.
4. Bailly R, Bosselut R, Zucman J, et al. DNA-binding and transcriptional activation properties of the EWS-FLI-1 fusion protein resulting from the t(11;22) translocation in Ewing sarcoma. Mol Cell Biol 1994;14:3230–41.
5. Ohno T, Rao V, Reddy E. EWS/Fli-1 chimeric protein is a transcriptional activator. Cancer Res 1993;53:5859–63.
6. Tanaka K, Iwakuma T, Harimaya K, et al. EWS-Fli1 antisense oligodeoxynucleotide inhibits proliferation of human Ewing's sarcoma and primitive neuroectodermal tumor cells. J Clin Invest 1997;99:239–47.
7. Maksimenko A, Lambert G, Bertrand JR, et al. Therapeutic potentialities of EWS-Fli-1 mRNA-targeted vectorized antisense oligonucleotides. Ann N Y Acad Sci 2003;1002:72–7.
8. Maksimenko A, Malvy C, Lambert G, et al. Oligonucleotides targeted against a junction oncogene are made efficient by nanotechnologies. Pharm Res 2003;20:1565–7.
9. Dohjima T, Lee NS, Li H, et al. Small interfering RNAs expressed from a Pol III promoter suppress the EWS/Fli-1 transcript in an Ewing sarcoma cell line. Mol Ther 2003;7:811–6.
10. Kovar H, Ban J, Pospisilova S. Potentials for RNAi in sarcoma research and therapy: Ewing's sarcoma as a model. Semin Cancer Biol 2003;13:275–81.
11. Chansky HA, Barahmand-Pour F, Mei Q, et al. Targeting of EWS/FLI-1 by RNA interference attenuates the tumor phenotype of Ewing's sarcoma cells *in vitro*. J Orthop Res 2004;22:910–7.
12. Lewis DL, Hagstrom JE, Loomis AG, et al. Efficient delivery of siRNA for inhibition of gene expression in postnatal mice. Nat Genet 2002;32:107–8.
13. McCaffrey AP, Meuse L, Pham TT, et al. RNA interference in adult mice. Nature 2002;418:38–9.
14. Song E, Lee SK, Wang J, et al. RNA interference targeting Fas protects mice from fulminant hepatitis. Nat Med 2003;9:347–51.
15. Filleur S, Courtin A, Ait-Si-Ali S, et al. siRNA-mediated inhibition of vascular endothelial growth factor severely limits tumor resistance to antiangiogenic thrombospondin-1 and slows tumor vascularization and growth. Cancer Res 2003;63:3919–22.
16. Duxbury MS, Matros E, Ito H, et al. Systemic siRNA-mediated gene silencing: a new approach to targeted therapy of cancer. Ann Surg 2004;240:667–74; discussion 675–6.
17. Soutschek J, Akinc A, Bramlage B, et al. Therapeutic silencing of an endogenous gene by systemic administration of modified siRNAs. Nature 2004;432:173–8.
18. Sioud M, Sorensen DR. Cationic liposome-mediated delivery of siRNAs in adult mice. Biochem Biophys Res Commun 2003;312:1220–5.
19. Zhang Y, Boado RJ, Pardridge WM. *In vivo* knockdown of gene expression in brain cancer with intravenous RNAi in adult rats. J Gene Med 2003;5:1039–45.
20. Zhang Y, Zhang YF, Bryant J, et al. Intravenous RNA interference gene therapy targeting the human epidermal growth factor receptor prolongs survival in intracranial brain cancer. Clin Cancer Res 2004;10:3667–77.
21. Schiffelers RM, Ansari A, Xu J, et al. Cancer siRNA therapy by tumor selective delivery with ligand-targeted sterically stabilized nanoparticle. Nucleic Acids Res 2004;32:e149.
22. Ge Q, Filip L, Bai A, et al. Inhibition of influenza virus production in virus-infected mice by RNA interference. Proc Natl Acad Sci U S A 2004;101:8676–81.
23. Urban-Klein B, Werth S, Abuharbeid S, et al. RNAi-mediated gene-targeting through systemic application of polyethylenimine (PEI)-complexed siRNA *in vivo*. Gene Ther 2005;12:461–6.
24. Bertrand JR, Pottier M, Vekris A, et al. Comparison of antisense oligonucleotides and siRNAs in cell culture and *in vivo*. Biochem Biophys Res Commun 2002;296:1000–4.
25. Minakuchi Y, Takeshita F, Kosaka N, et al. Atelocollagen-mediated synthetic small interfering RNA delivery for effective gene silencing *in vitro* and *in vivo*. Nucleic Acids Res 2004;32:e109.
26. Takei Y, Kadomatsu K, Yuzawa Y, et al. A small interfering RNA targeting vascular endothelial growth factor as cancer therapeutics. Cancer Res 2004;64:3365–70.
27. Pille JY, Denoyelle C, Varet J, et al. Anti-RhoA and anti-RhoC siRNAs inhibit the proliferation and invasiveness of MDA-MB-231 breast cancer cells *in vitro* and *in vivo*. Mol Ther 2005;11:267–74.
28. Layzer JM, McCaffrey AP, Tanner AK, et al. *In vivo* activity of nuclease-resistant siRNAs. RNA 2004;10:766–71.
29. Braasch DA, Paroo Z, Constantinescu A, et al. Biodistribution of phosphodiester and phosphorothioate siRNA. Bioorg Med Chem Lett 2004;14:1139–43.
30. Gonzalez H, Hwang SJ, Davis ME. New class of polymers for the delivery of macromolecular therapeutics. Bioconjug Chem 1999;10:1068–74.
31. Pun SH, Davis ME. Development of a nonviral gene delivery vehicle for systemic application. Bioconjug Chem 2002;13:630–9.
32. Davis ME, Pun SH, Bellocq NC, et al. Self-assembling nucleic acid delivery vehicles via linear, water-soluble, cyclodextrin-containing polymers. Curr Med Chem 2004;11:179–97.
33. Bellocq NC, Pun SH, Jensen GS, et al. Transferrin-containing, cyclodextrin polymer-based particles for tumor-targeted gene delivery. Bioconjug Chem 2003;14:1122–32.
34. Gatter KC, Brown G, Trowbridge IS, et al. Transferrin receptors in human tissues: their distribution and possible clinical relevance. J Clin Pathol 1983;36:539–45.
35. Pun SH, Tack F, Bellocq NC, et al. Targeted delivery of RNA-cleaving DNA enzyme (DNAzyme) to tumor tissue by transferrin-modified, cyclodextrin-based particles. Cancer Biol Ther 2004;3:641–50.
36. Sledz CA, Holko M, de Veer MJ, et al. Activation of the interferon system by short-interfering RNAs. Nat Cell Biol 2003;5:834–9.
37. Bridge AJ, Pebernard S, Ducraux A, et al. Induction of an interferon response by RNAi vectors in mammalian cells. Nat Genet 2003;34:263–4.
38. Heidel JD, Hu S, Liu XF, et al. Lack of interferon response in animals to naked siRNAs. Nat Biotechnol 2004;22:1579–82.
39. Bahner I, Kearns K, Hao QL, et al. Transduction of human CD34$^+$ hematopoietic progenitor cells by a retroviral vector expressing an RRE decoy inhibits human immunodeficiency virus type 1 replication in myelomonocytic cells produced in long-term culture. J Virol 1996;70:4352–60.
40. Challita PM, Skelton D, el-Khoueiry A, et al. Multiple modifications in *cis* elements of the long terminal repeat of retroviral vectors lead to increased expression and decreased DNA methylation in embryonic carcinoma cells. J Virol 1995;69:748–55.
41. Wang X, Rosol M, Ge S, et al. Dynamic tracking of human hematopoietic stem cell engraftment using *in vivo* bioluminescence imaging. Blood 2003;102:3478–82.
42. Rehemtulla A, Stegman LD, Cardozo SJ, et al. Rapid and quantitative assessment of cancer treatment response using *in vivo* bioluminescence imaging. Neoplasia 2000;2:491–5.
43. Vooijs M, Jonkers J, Lyons S, et al. Noninvasive imaging of spontaneous retinoblastoma pathway-dependent tumors in mice. Cancer Res 2002;62:1862–7.
44. Zhang J, Hu S, Schofield DE, et al. Selective usage of D-type cyclins by Ewing's tumors and rhabdomyosarcomas. Cancer Res 2004;64:6026–34.
45. Vormoor J, Baersch G, Decker S, et al. Establishment of an *in vivo* model for pediatric Ewing tumors by transplantation into NOD/scid mice. Pediatr Res 2001;49:332–41.
46. Sorensen DR, Leirdal M, Sioud M. Gene silencing by systemic delivery of synthetic siRNAs in adult mice. J Mol Biol 2003;327:761–6.
47. Hasuwa H, Kaseda K, Einarsdottir T, et al. Small interfering RNA and gene silencing in transgenic mice and rats. FEBS Lett 2002;532:227–30.
48. Miyagishi M, Taira K. Development and application of siRNA expression vector. Nucleic Acids Res Suppl 2002;2:113–4.
49. Pekarik V, Bourikas D, Miglino N, et al. Screening for gene function in chicken embryo using RNAi and electroporation. Nat Biotechnol 2003;21:93–6.
50. Hemann MT, Fridman JS, Zilfou JT, et al. An epiallelic series of p53 hypomorphs created by stable RNAi produces distinct tumor phenotypes *in vivo*. Nat Genet 2003;33:396–400.
51. Rubinson DA, Dillon CP, Kwiatkowski AV, et al. A lentivirus-based system to functionally silence genes in primary mammalian cells, stem cells and transgenic mice by RNA interference. Nat Genet 2003;33:401–6.
52. Tanaka T, Shiramoto S, Miyashita M, et al. Tumor targeting based on the effect of enhanced permeability and retention (EPR) and the mechanism of receptor-mediated endocytosis (RME). Int J Pharm 2004;277:39–61.
53. Hornung V, Guenthner-Biller M, Bourquin C, et al. Sequence-specific potent induction of IFN-α by short interfering RNA in plasmacytoid dendritic cells through TLR7. Nat Med 2005;11:263–70.
54. Judge AD, Sood V, Shaw JR, et al. Sequence-dependent stimulation of the mammalian innate immune response by synthetic siRNA. Nat Biotechnol 2005;23:457–62.
55. Ma Z, Li J, He F, et al. Cationic lipids enhance siRNA-mediated interferon response in mice. Biochem Biophys Res Commun 2005;330:755–9.